Permeation behavior of Polysulfone membranes modified by fully organic Layer by Layer assemblies.

Journal:	*Industrial & Engineering Chemistry Research*
Manuscript ID:	ie-2013-02942g.R1
Manuscript Type:	Article
Date Submitted by the Author:	n/a
Complete List of Authors:	Tylkowski, Bartosz; Universitat Rovira i Virgili, Carosio, Federico; Politecnico di Torino, Castañeda, Joandiet; Universitat Rovira i Virgili, Alongi, Jenny; Politecnico di Torino, Garcia-Valls, Ricard; Universitat Rovira i Virgili, Malucelli, Giulio; Politecnico di Torino, Giamberini, Marta; University Rovira i Virgili, Chemical Engineering

Permeation behavior of Polysulfone membranes modified by fully organic Layer by Layer assemblies.

Bartosz Tylkowski[1,2], Federico Carosio[3], Joandiet Castañeda[1], Jenny Alongi[3], Ricard García-Valls[1], Giulio Malucelli[3], Marta Giamberini[1] *

[1] Universitat Rovira i Virgili, Departament de Enginyeria Química, Av. Països Catalans, 26 - 43007 Tarragona Spain

[2] *Centre Tecnologic de la Quimica de Catalunya, Carrer de Marcelli Domingo, s/n Campus Sescelades, 43007 Tarragona Spain*

[3] Department of Applied Science and Technology, Politecnico di Torino, Viale T. Michel 5, 15121 Alessandria, Italy

* corresponding author, Phone: +34977558174, Fax: +34977559621, e-mail: marta.giamberini@urv.net

Abstract

This paper investigates the effect of the deposition of Layer by Layer assemblies on the swelling, permeability and anthracene rejection of polysulfone (PSf) membranes obtained through phase inversion precipitation technique. More specifically, these latter have been dip-coated on one side with a completely organic assembly (made of polyacrylic acid/branched polyethyleneimine bi-layers), varying the number of deposited bi-layers from 10 to 20. Prior the deposition, the surface of the polysulfone membranes has been subjected to plasma activation. Static contact angle, Scanning Electron Microscopy and attenuated total reflectance infrared spectroscopy measurements have been exploited for evaluating the modification of polysulfone after the LbL deposition, as well as the homogeneity of the distribution and coverage of the coatings on the polymeric substrate. The swelling of both untreated and LbL-treated membranes has been evaluated in three different solvents, i.e. methanol, isopropanol and n-hexane; subsequently, the permeation features of the treated membranes toward these solvents have been assessed and correlated with the presence of the deposited assembly; finally, the retention of anthracene in its n-hexane solutions has been evaluated.

Keywords: Layer by Layer assembly; polysulfone membranes; swelling; permeability; anthracene rejection.

1. Introduction

Polysulfone (PSf) is a well-known polymer broadly used in the industry. It has very good chemical and thermal stability and allows easy manufacturing of membranes with reproducible properties and controllable size of pores down to 40 nanometers. For this reason, it has been extensively used as a base material for ultrafiltration membranes in applications like hemodialysis, waste water recovery, food and beverage processing and gas separation.[1, 2] In order to enhance their final properties, PSf membranes can be subjected to different surface modifications, among which, the *layer-by-layer* (LbL) approach seems to be very effective.

LbL technique is a step-by-step build-up process that falls in the category of self-assembled coatings and can be exploited for quite easily modifying the surface of different plastic substrates. Although this method has been initially described in 1966[3], it has been rediscovered and optimized decades later[4-7]; nowadays, LbL applications include membranes for direct methanol fuel cells[8], polymer catalytic electrodes[9], field-effect transistors[10], anti-reflection[11], antibacterial [12] or electrical conductive coatings[13], and humidity sensors[14]. In addition, this method has been also used for conferring flame retardancy to plastics and textiles[15-19].

The main advantages of LbL with respect to more traditional thin film deposition techniques include: i) facile incorporation of functional species, ii) processing under ambient conditions (e.g. room temperature, atmospheric pressure) and iii) low environmental impact (water is mostly used as solvent and the concentrations of the solutions/dispersions are usually below 1 wt.-%).

The technique was introduced in 1991 for polyanion/polycation films in order to obtain the so-called *polyelectrolyte multilayers*[7] and subsequently extended to inorganic nanoparticles[20]. It simply consists in alternatively immersing a chosen substrate into diluted polyelectrolyte

solutions (or nanoparticle dispersions) bearing opposite electrical charges; as a results of this procedure, a structure of positively and negatively charged layers (commonly defined *bi-layers*), piled up on the substrate surface, is obtained.

A general scheme of the LbL process is shown in Figure 1: due to the electrostatic attraction that occurs between each layer during the building-up of the assembly, the strong resulting interactions allow creating a well packed architecture; furthermore, the process can be easily adjusted to any kind of substrate, irrespective of its size and topology, so that it can be used for treating plates, thin films and even textiles and foams.

Despite the number of papers concerning the use of LbL architectures for enhancing the barrier properties of plastic films toward different gases[21-23], or for designing new generations of proton exchange membranes[24] their application for tuning the selectivity/retention features of membranes toward organic solvents is relatively new. For instance, LbL assembly has been proposed for fouling and biofouling reduction[20, 25, 26], for lowering methanol and oxygen cross-over in Nafion membranes[27-30], for improving the performances in forward osmosis[31] and for enhancing selectivity and flux in nanofiltration[32-34].

Therefore, in the present work, polysulfone films, prepared by means of phase inversion precipitation technique, have been LbL-treated with 10 and 20 bi-layers of polyacrylic acid/branched polyethyleneimine, aiming to assembly a fully organic coating on one side of the polymer surface, thus obtaining asymmetric membranes.

First of all, the growth of the obtained architectures has been assessed through scanning electron microscopy (SEM) and FTIR-ATR spectroscopy measurements.

Unmodified and modified membranes were tested with respect to their swelling properties, organic solvent permeability and anthracene rejection. In this way, it was assessed that the

performances of PSf membranes can be improved by LbL treatments and that these modified materials can be applied to nanofiltration also as membranes resistant to organic solvents.

2. Experimental Section

2.1 Materials

Polysulfone, PSf (Aldrich, M_w ~35000 by LS), Anthracene (Sigma Aldrich) N,N dimethylformamide, DMF (Panreac, 99,8% PS), isopropanol (Panerac, QP), n-hexane (Scharlau, 99% reagent grade), methanol (Scharlau, reagent grade), were used as received.

Poly(acrylic acid) (PAA) and branched polyethyleneimine (BPEI) were purchased from Sigma Aldrich (Milwaukee, WI) and used, without any further modification, for preparing 0.1 or 0.2 wt.% aqueous solutions, respectively, employing 18.2 MΩ deionized water supplied by a Q20 Millipore system (Milano, Italy). The pH values of PAA and BPEI solutions were set at 4 and 10, respectively.

2.2. Preparation of Polysulfone membranes

Flat sheet polysulfone membranes were prepared by phase inversion precipitation (PIP) process, in which a homogenous polymer solution is cast on a suitable support and immersed in a coagulation bath containing a non-solvent. Precipitation occurs due to exchange of solvent and nonsolvent molecules in contact with the polymer. In order to prepare asymmetric membranes, PSf polymer was dissolved in DMF at 22±2 ºC by stirring for 8 hours to obtain 15 wt% homogeneous solution. Next, the solution was cast on a glass plate by means of a custom-made casting knife (gap 200 μm) connected with a K Paint Applicator (R K Print Coat Instruments

Ltd, UK.). Then, the cast films were coagulated in a bath containing distilled water as a non-solvent. After primarily phase separation and formation, the membranes were stored in water for 24 h to guarantee complete phase separation. This allows the water soluble components in the membrane to be leached out. As the final stage, the membranes were dried by placing them between two sheets of filter paper for 24 h at room temperature.

Hereafter, the obtained membranes will be coded as M0, M1 and M2, where 0 stands for untreated, while 1 and 2 refer to the deposition of 10 and 20 bi-layer (BL) assemblies respectively.

2.3. Layer by layer deposition

Prior to the layer-by-layer deposition, M0 films were activated with cold plasma (oxygen, 10 cm^3/min and argon, 10 cm^3/min) using a 40 kHz Pico 1.1.2 semi-automatic controlled system (Diener Electronic GmbH), operating at 50 W for 5 min.

After the plasma treatment, the polysulfone substrates were coupled two by two and alternately immersed into the positively (BPEI) and the negatively (PAA) charged baths, thus performing the LbL treatment just on one side of each film (dipping apparatus: KSV DX2S-500 LM dip-coater, Helsinki, Finland); after each adsorption step, the substrates were washed with deionized water by static dipping for 5 min. The immersion period for the first couple of layers was set at 10 min, in order to promote uniformity and stability; the subsequent layers were obtained after 5 min dipping. The process was repeated until 10 and 20 BL were built on each specimen type.

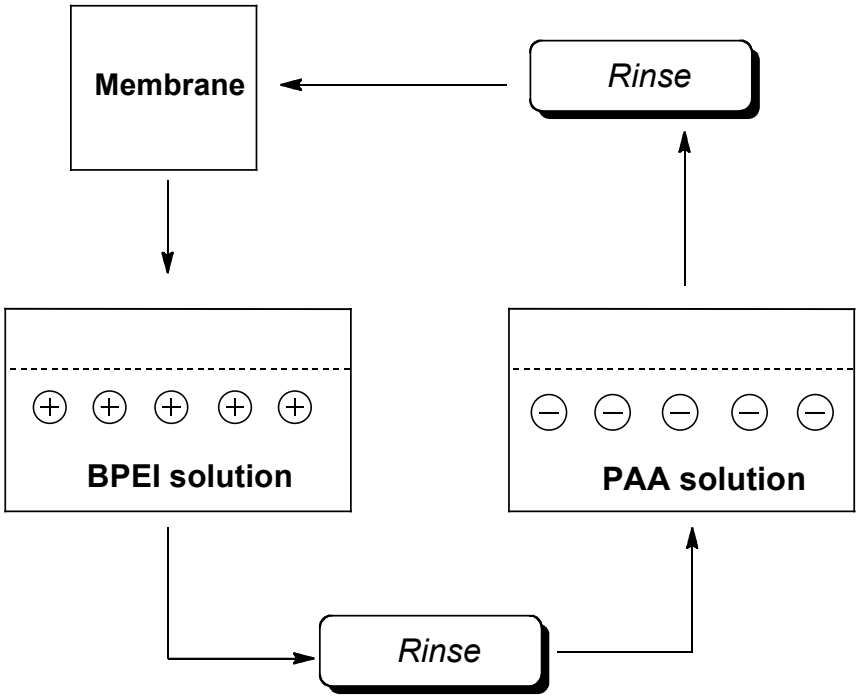

Figure 1. Schematic of the LbL deposition process

2.2 Characterization Techniques

The growing of the coatings deposited through LbL on polysulfone was assessed by Attenuated Total Reflectance (ATR) spectroscopy. ATR Spectra were recorded at room temperature in the range 4000-600 cm^{-1} (16 scans and 4 cm^{-1} resolution), using a Frontier FT-IR/FIR spectrophotometer, equipped with a Universal ATR Sampling Accessory (diamond crystal: depth of penetration 1.66μm, as stated by the producer). Both the untreated and LbL-treated membranes were imaged using a scanning electron microscope (SEM, model 1450VP by LEO) equipped with a back scattered electron detector. Small pieces (5 x 5 mm^2) were cut and fixed to conductive adhesive tapes and gold-metallized. The average thickness of the membrane and of the BL assemblies (10 measures) was calculated from SEM micrographs of the cross-sections, using an Image-ProPlus 5 software (Media Cybernetics Inc., USA). The membrane

porosity was evaluated by means of IFME® software on the cross-section SEM micrographs[35]. At least 20 measurements were replicated for ensuring reproducibility.

The flux and rejection experiments were carried out using a self-made stainless steel cross-flow nanofiltration apparatus containing a disk membrane module. The effective membrane area in the module is 12.6 cm^2. Figure 2 shows the flow diagram of the cross-flow nanofiltration apparatus. The feed to the filtration cells is supplied by a piston pump and damped by a pulsation dampener before the membrane cells. During the experiments, the temperature of feed/retentate and permeate, as well as pressure in the membrane cells are controlled.

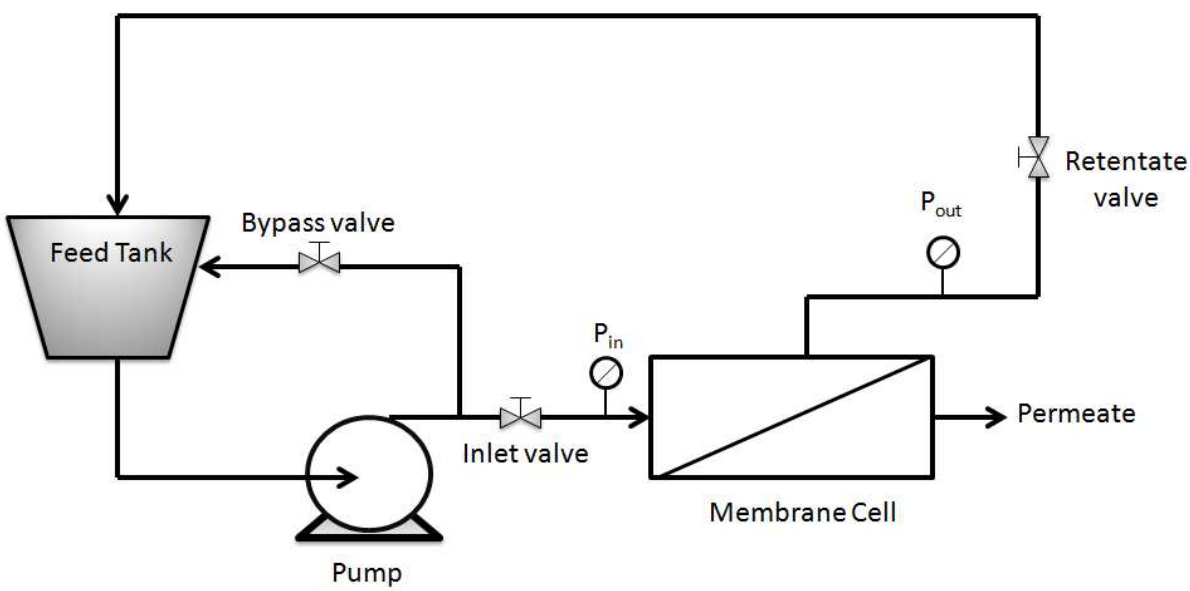

Figure 2. Flow diagram of the cross-flow nanofiltration apparatus.

The flux and rejection experiments were performed using the following procedure: after the initial insertion of the membrane films in the cells with the LbL treated side towards the feed, the plant was run first for 15 min without feed pressure in order to condition the system and hence with for 15 min with 10 bar feed pressure, to reach a steady state permeate flux and to complete

the initial membrane compaction. As far as experiments at 10 bar pressure are concerned, whenever the solution in the feed tank was changed, the entire apparatus was washed three times with the new solvent before continuing the experiments. In addition, the system was run with 10 bar feed pressure for at least 15 min in order to facilitate the removal of the former solvent. Then, compaction at 10 bar feed pressure was done again until steady state conditions were reached.

Membrane performances were evaluated on the basis of the solvent flux and rejection experiments[36]. The flux (J) through the membrane can be described by the following equation:

$$J = \frac{V}{A\Delta t} \qquad (1)$$

where V is the permeate volume, A is the membrane area and Δt is the permeation time. Anthracene rejection ratio was calculated by the following equation:

$$R(\%) = \left(1 - \frac{C_p}{C_f}\right) \cdot 100 \qquad (2)$$

where C_p and C_f (mg/mL) are the concentrations of permeate and feed solutions, respectively. Anthracene concentration was determined spectrophotometrically, by measuring its absorbance at 375 nm [37], with a UV–Vis spectrophotometer (U-2800 Hitachi, Japan) upon calibration.

The wettability of the surfaces after the LBL deposition was assessed by static contact angle measurements, using a KSV CAM 200 apparatus (Nordtest, Italy), using double distilled water (Sigma – Aldrich) as solvent.

Swelling experiments were accomplished for evaluating the chemical resistance of the membranes.

Swelling (*S*w)[38] was referred to the weight increase due to solvent absorption, according to the following equation:

$$S_w = \left(\frac{W_w - W_d}{W_d}\right) \cdot 100 \qquad (3)$$

where W_d and W_w are the weights of dry and wet membrane samples, respectively.

In order to investigate influence of LbL modification on PSf membrane swelling and resistance behaviors, a study was performed using the same self-made stainless steel cross-flow nanofiltration apparatus, previously described in flux and rejection experiments. During the swelling study, the apparatus was filled in with appropriate solvent and only modified membrane surface was exposed to it for 72 h, at 24°C, at atmospheric pressure, while during the solvent resistance experiments 10 bar pressure was applied. All swelling experiments were replicated with at least three samples of each membrane and the values averaged.

3. Results and discussion

3.1 Surface characterization of the LbL assemblies

ATR spectroscopy has been exploited for assessing the growth of the deposited coatings on polysulfone films. Figure 3 shows the ATR spectrum of untreated PSf membrane: aromatic in-plane ring stretching vibrations occur in the region from 1620 to 1430 cm^{-1}. A C–H symmetric deformation vibration of $C(CH_3)_2$ is shown as two weak-medium bands in the range of 1385–1350 cm^{-1}. Aryl-O-aryl group has a characteristic strong band centered at 1240 cm^{-1}, associated with the C–O–C asymmetric stretching vibration. The asymmetric O=S=O stretching vibration occur in the 1350–1280 cm^{-1} region and the band due to the symmetric stretching vibration within 1180 and 1145 cm^{-1}. The band at 835 cm^{-1} results from the in-phase out-of-plane

hydrogen deformation for parasubstituted phenyl groups [39]. Figure 4 compares the collected spectra of polysulfone treated by 10 and 20 BL with that of the untreated substrate. It is worth noticing that the typical signals of the PSf are completely hidden by the layer by layer deposition, irrespective of the number of deposited bilayers. Indeed, some characteristic peaks of PAA can be distinguishable (namely, at 1470 cm^{-1}, s $\nu(COO^-)$ asymmetric and symmetric); furthermore, the strong band located at 1580 cm^{-1} may be the result of an overlapping between strong -COO- asymmetric stretching and medium-to-strong NH_2 and NH_3^+ stretching.[40]

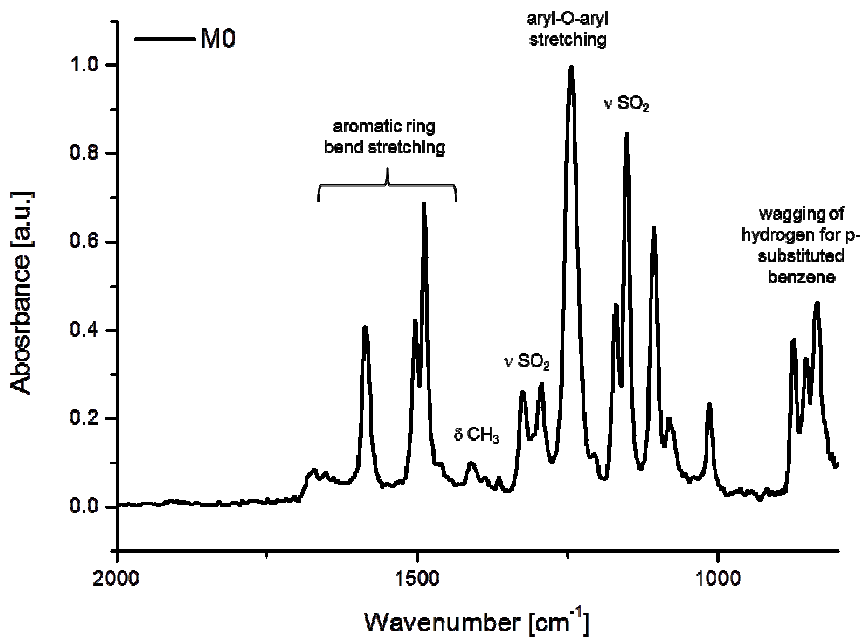

Figure 3: ATR spectrum of untreated PSf membrane

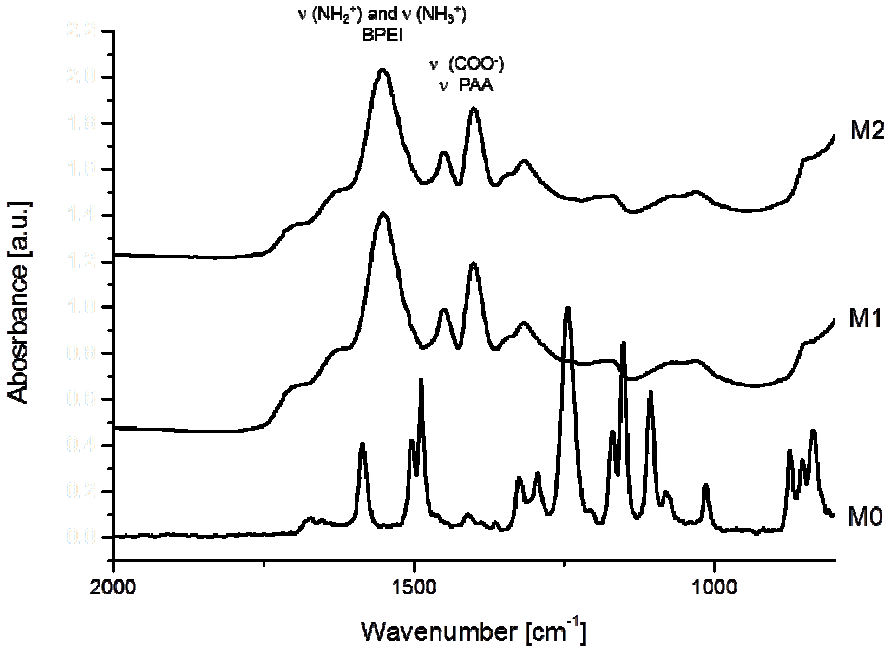

Figure 4. ATR spectra of untreated and LbL-treated PSf membranes

In order to confirm this hypothesis, SEM analyses have been used to investigate the morphology of deposited coatings. Figure 5 shows the typical morphology of LbL-treated and untreated substrates.

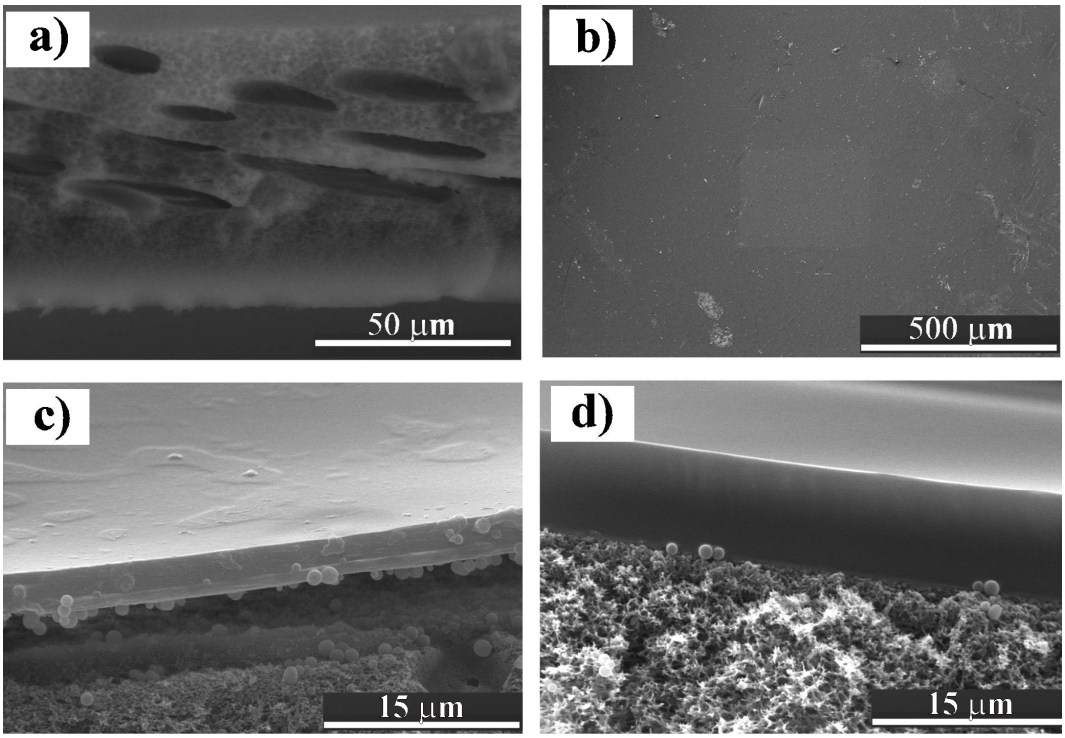

Figure 5. SEM micrographs of M0 cross-section (a), M0 surface (b), M1 cross-section (c) and M2 cross-section (d).

Figure 5a shows the typical SEM micrographs of untreated M0 membrane: it is asymmetric and exhibits macrovoids, as it consists of a dense skin layer and a spongy-like porous inner structure. It is well known that, in a phase separation process, liquid−liquid demixing and polymer−liquid demixing in a polymer/solvent/ nonsolvent system play a very important role in determining the membrane structure[41]. Niwa et al. [42] reported that the liquid−liquid exchange rate between the solvent and the nonsolvent has a great influence on the skin layer thickness and on the membrane structure. Asymmetric membranes formed by delayed demixing possess a dense skin layer supported by a sponge-type structure, while the membranes formed by instantaneous demixing exhibit an ultrathin top skin layer supported by a finger-type structure. The delay time is about one second or less for rapid demixing conditions, while for delayed

demixing the precipitation time can range from seconds to minutes. The asymmetric morphology with macrovoids is found when membranes are prepared by immersion precipitation using DMF/water as the solvent/non-solvent pair [43], as in the present study. Indeed, SEM micrographs of M0 membrane (Figure 5a) show a smooth surface with the presence of defects. Conesa et al.[44] and Smolders et al.[45] hypothesized that in PSf/DMF/H_2O system the macrovoid structure is a consequence of the fast polymer precipitation rate that arises from a high miscibility between the solvent/nonsolvent pair. In addition, the Monte Carlo diffusion model described by Termonia[46] theorizes that the solvent/non-solvent interaction parameter is the main controlling step in the formation of macrovoids. More specifically, this latter was ascribed to non-solvent penetration through skin defects. The faster solvent exchange for non-solvent through the defects was thought to be responsible for the growth of macrovoids. On the other hand, when the solvent/non-solvent pair was chloroform/methanol, regardless of the membrane thickness, macrovoids were never detected due to the slower exchange of chloroform with methanol.

Membrane thickness, calculated by Image-ProPlus 5® software on ESEM micrographs, was around 71.6 (±0.8) μm. The pore mean size of the membrane as well as its asymmetry yielded values of ca. 4.26 (±0.03) μm and 19%, respectively; pore sizes ranged between 12.4 and 0.10 μm.

Figures 5c and d show the cross-section morphologies of M1 and M2 membranes, respectively. The thicknesses of the LbL assembly were around 3.1 (±0.1) μm (M1) and 5.1 (±0.3) μm (M2): they can be be ascribed to the exponential growth of the coating combined with the adopted deposition times. Indeed, it has been reported in the literature that BPEI and PAA (at pH 10 and 4, respectively) can yield an exponential growth of the LbL films.[22, 47] This has been explained on the basis of an “in and out” diffusion mechanism where the polymer chains not

only adsorb on the LbL film surface but also interpenetrate into inner layers, thus exponentially increasing the total film thickness.

Furthermore, it can be easily observed that the Layer-by-Layer deposition is able to homogeneously cover the surface, irrespective of the number of deposited bilayers. The pore mean size of the modified membranes was similar to that of M0 counterpart (i.e. about 4.25 μm). This finding suggests that positively and negatively charged aqueous solutions do not penetrate the polysulfone membrane during the repeated immersion steps, because of the high hydrophobic character of the membrane, as assessed by static contact angle measurements with water (ϑ=98°, Table 1). This value, slightly higher than those reported in the literature [48], can be ascribed to the different solvent–non solvent interactions during the phase-inversion process, as well as to the different conditions adopted for the membrane preparation. In addition, as expected, the LbL deposition of a coating made of polar layers (BPEI and PAA) is capable of significantly reducing the water contact angle, i.e. increasing its hydrophilicity. (Table 1) It is worth noticing that the contact angle decrease is independent of the deposited BL number.

Resistance tests were carried out on M0, M1 and M2 membranes in order to assess their stability in water, methanol, isopropanol and n-hexane after 72h exposure, with the experimental setup previously described. It was observed that M1 and M2 LbL assemblies readily dissolved into water: indeed, the deposited layers were prepared starting from water solutions. At variance, all the tested membranes showed an excellent stability in the three organic solvents.

The swelling values of the different types of membranes are collected in Table 1. M0 exhibits the highest degree of swelling in all the organic solvents, while M1 and M2 membranes show a different behavior: indeed, their swelling in methanol and isopropanol is approximately 40 and 60% lower than M0. From an overall point of view, both the dielectric constant of the solvent

and the difference in solubility parameters between polymer and solvent govern the swelling behavior.[38] Membrane swelling is higher in polar solvents like methanol (polarity index =76.2 (water polarity index = 100)) due to its high dielectric constant (ε = 32.6), and lower with nonpolar solvents like n-hexane (polarity index = 0.9; ε = 1.9). The same trend is observed by comparing the membrane swelling in methanol and isopropanol (polarity index =54; ε = 18.3).

In all cases, swelling decreases on going from M0 to M2. In LbL treated membranes, the deposited assembly limits the permeation of the used wetting solvents: this effect is more evident on increasing the number of deposited bilayers, which ensures a more homogeneous coverage of the membrane surface.

Table 1. Static contact angle with water and membrane swelling[a] at 22±2ºC.

Membrane batch no	Static contact angle (°)	Weight swelling (%)		
		methanol	isopropanol	n-hexane
M0	98± 2	375±8	335±7	50±1
M1	45± 2	218±4	200±3	44±1
M2	45± 2	150±1	137±2	31±1

[a]Percentage of weight increase after exposure to the different solvents for 72 h

M0 and M1 membrane performances were evaluated using the three pure solvents, as well as an anthracene solution in n-hexane (0.01M); M2 membrane could not be tested due to the tendency of the LbL assembly to form cracks.

Tables 2 and 3 present flux values and some of the physical properties[49] of the used solvents. First of all, it is worthy to note that the fluxes of organic solvents decrease after the LbL deposition irrespective of the type of solvent used.

The description of transport mechanism to non-aqueous systems is complex and depends on the structures and properties of the solvents.[50] Membrane-solvent interactions can be expected to

vary with changes in such solvent properties as viscosity, dielectric constant, molecular size, dipole moment, solubility parameter and surface tension. According to Machado et al.[51] and Bhanushali et al.[52], viscosity is the key parameter affecting solvent flow through nanofiltration membranes. Except for the anomalous behavior of water [53], all the other solvents show a consistent increase in flux when their viscosity decrease.

Comparing the flux values for isopropanol and n-hexane, the flux of pure isopropanol is lower than that of n-hexane, because of the higher viscosity of the former and its higher dielectric constant. These results indicate that the transport of isopropanol and n-hexane through PSf membranes is governed by a viscous flow permeation mechanism. The same mechanism was described by Schmidt et al. [54], who investigated the influence of the physical properties of n-hexane and isopropanol on the transport mechanism through Starmem™ 122, a commercial polyimide-based membrane.

Comparing the flux values for n-hexane and methanol, the permeate flux of this latter is higher with respect to n-hexane. This finding indicates that, in this case, permeation is not dominated by viscosity: indeed, the higher solubility parameter of methanol with respect to n-hexane results in a greater affinity between methanol and the membranes. Furthermore, the flux values decrease moving from methanol to isopropanol, i.e by lengthening the alcohol structure by additional CH_2 groups. This result is consistent with literature data, which clearly show that flux decreases with increasing molecular length, irrespective of the transport mechanism[55,53]. Machado et al. [51] observed that flux values for alcohol molecules decrease with changes in surface tension. The addition of one *C* atom to the alcoholic structure increases the surface tension by a constant factor of approximately 1.03. In addition, the viscosity of small alcohol molecules ($C<3$) is enhanced by ca. 0.51–0.55 and by 0.77 for large molecules ($C>3$).

The toxicity of anthracene, a common polycyclic aromatic hydrocarbon (PAH), has been extensively assessed under environmentally realistic conditions. Polycyclic aromatic hydrocarbons are ubiquitous and persistent, for instance, in contaminated soils, waters, sediments and exhibit a significant risk to the environment and human health[56]. They are generally formed as byproducts of the incomplete combustion of organic material including fossil fuels, wood, and refuse, and are emitted from internal combustion and diesel.[57] Because of its low molecular weight compared to most of the other PAHs, anthracene has a higher solubility and can be found at significant levels in the environment. Therefore, it is important to develop new cheap and environmentally friendly methods for its separation or concentration.

In order to assess the effectiveness of the Layer by Layer treatment on the rejection features of M1 membranes, the anthracene concentrations in permeate and retentate were analyzed and its rejection was calculated according to Eq. 2. As can be seen in Table 2, about 90% anthracene passes through the asymmetric structure of the untreated polysulfone membrane; at variance, only 32% of the polynuclear aromatic hydrocarbon diffuses through the dense layer of the 10 BL treated membrane. This finding is in agreement with Su et al.[58], who tested negatively charged polysulfone ultrafiltration membranes treated with bilayers of poly(diallyl-dimethylammonium chloride) and poly(styrene sulfonate).

Recently, Ahmadiannamini et al. studied rejection of rose bengale (RB) from RB/isopropanol feed solution using multilayered polyelectrolyte complexes membrane based on LBL method from poly(diallyldimethylammonium chloride) (PDDA) as polycation.[34] Based on high, i.e. >99 %, retention value of RB from RB/isopropanol, with high flux value 1.57 Lm^{-2} h^{-1} bar^{-1}, authors strongly recommend these LbL membranes as a promising solvent resistant nanofiltration (SRNF) membrane. In our investigation, instead of a high molecular weight compound as RB

(MW 1017 g/mol), we tested an anthracene/isopropanol feed solution. Despite anthracene low molecular weight (MW 178 g/mol), 6 times lower than RB, we were successful to reject 68% of it with 29.6 Lm^{-2} h^{-1} bar^{-1} flux. It is worth to underline, that this flux value is approximately 60 times higher than the flux value of RB/isopropanol feed solution through SRNF modified PSf/SPEEK membranes (0.47 Lm^{-2} h^{-1} bar^{-1}) reported by Li et al.[33] Therefore, the combination of high retention of very low molecular weight compound and very high fluxes of the prepared 10 LbL/PSf films make them very promising for commercial SRNF.

Table 2. Flux of organic solvents and anthracene rejection through M0 and M1 membranes at 10 bar and 22±2ºC.

Membrane type	J (Lm^{-2} h^{-1})			Rejection (%)
	isopropanol	n-hexane	methanol	Anthracene
M0	370 ± 8	498 ± 13	715 ± 15	11 ± 1
M1	296 ± 11	433 ± 5	540 ± 16	68 ± 1

Table 3. Physical properties of the organic solvents used[49]

Solvent	Polarity index[1]	ε at 20°C	Solubility parameter[59] ($MPa^{0.5}$)	Surface tension (mN/m)	Viscosity (mPa s)
methanol	76.2	32.6	29.7	22.5	0.59
isopropanol	54.6	18.3	23.8	21.7	2.00
n-hexane	0.90	1.90	14.9	18.4	0.31

[1] Water polarity index: 100

4. Conclusions

PSf membranes were successfully LbL-treated, using poly(acrylic acid) and branched polyethyleneimine layers. ATR spectroscopy confirmed the deposition of homogeneous coatings on the membrane. Their thickness ranged between 3 and 5 μm, for 10 and 20 BL assemblies, respectively. The swelling of the membranes in methanol, isopropanol and n-hexane was found to decrease with increasing the number of deposited bi-layers. Permeation tests showed that the transport of isopropanol and n-hexane through PSf membranes is governed by a viscous flow permeation mechanism; at variance, moving from methanol to isopropanol, i.e by lengthening the alcohol structure by additional CH_2 groups, the flux decreases with increasing molecular length, irrespective of the transport mechanism. The anthracene rejection evaluated on 10 bi-layers coated membranes was found to increase up to 68% as a consequence of LbL treatment, as compared to 11% of untreated PSf, with 29.6 Lm^{-2} h^{-1} bar^{-1} flux. These results suggest that the LbL treatment can widen the application of PSf membranes to new fields such as organic solvents nanofiltration or concentration/separation of cancerogenic (i.e. anthracene) as well as biological active compounds.

ACKNOWLEDGEMENTS

The authors would like to gratefully acknowledge LLP/ERASMUS Program between Universitat Rovira i Virgili and Politecnico di Torino.

Literature cited

1. Mulder, M. *Basic Principles of Membrane Technology*. Kluwer Academic Publishers: The Netherlands, 1997.

2. Esser-Kahn, A. P.; Odom, S. A.; Sottos, N. R.; White, S. R.; Moore, J. S. Triggered Release from Polymeric Microcapsules. *Macromolecules* **2011,** *44*, 5539-5553.

3. Iler, R. K. Multilayers of colloidal particles. *J Colloid Interface Sci* **1966,** *21*, 569-594.

4. Ariga, K.; Hill, P.; Ji, Q. Layer-by-layer assembly as a versatile bottom-up nanofabrication technique for exploratory research and realistic application. *Phys Chem Chem Phys* **2007,** *9*, (19), 2319-2340.

5. Hammond, P. T. Form and Function in Multilayer Assembly: New Applications at the Nanoscale. *Adv Materials* **2004,** *16*, 1271-1293.

6. Decher, G.; Hong, J.-D. Buildup of ultrathin multilayer films by a self-assembly process, 1 consecutive adsorption of anionic and cationic bipolar amphiphiles on charged surfaces. *Makromolekulare Chemie. Macromolecular Symposia* **1991,** *46*, (1), 321-327.

7. Decher, G., Polyelectrolite Multilayers, an Overview. In *Multilayer Thin Films, Sequential assembly of nanocomposite materials*, G Decher, J. B. S., Ed. Wiley VCH: Weinheim, 2003; pp 1-46.

8. Jiang, S. P.; Liu, Z.; Tian, Z. Q. Layer-by-Layer Self-Assembly of Composite Polyelectrolyte–Nafion Membranes for Direct Methanol Fuel Cells. *Advanced Materials* **2006,** *18*, (8), 1068-1072.

9. Farhat, T. R.; Hammond, P. T. Engineering Ionic and Electronic Conductivity in Polymer Catalytic Electrodes Using the Layer-By-Layer Technique. *Chemistry of Materials* **2005,** *18*, (1), 41-49.

10. Cui, T.; Liu, Y.; Zhu, M. Field-effect transistors with layer-by-layer self-assembled nanoparticle thin films as channel and gate dielectric. *Applied Physics Letters* **2005,** *87*, (18), 183105.

11. Hiller, J. A.; Mendelsohn, J. D.; Rubner, M. F. Reversibly erasable nanoporous anti-reflection coatings from polyelectrolyte multilayers. *Nat Mater* **2002,** *1*, (1), 59-63.

12. Falentin-Daudré, C.; Faure, E.; Svaldo-Lanero, T.; Farina, F.; Jérôme, C.; Van De Weerdt, C.; Martial, J.; Duwez, A.-S.; Detrembleur, C. Antibacterial Polyelectrolyte Micelles for Coating Stainless Steel. *Langmuir* **2012,** *28*, (18), 7233-7241.

13. Luther, J. M.; Law, M.; Song, Q.; Perkins, C. L.; Beard, M. C.; Nozik, A. J. Structural, Optical, and Electrical Properties of Self-Assembled Films of PbSe Nanocrystals Treated with 1,2-Ethanedithiol. *ACS Nano* **2008,** *2*, (2), 271-280.

14. Nohria, R.; Khillan, R. K.; Su, Y.; Dikshit, R.; Lvov, Y.; Varahramyan, K. Humidity sensor based on ultrathin polyaniline film deposited using layer-by-layer nano-assembly. *Sensors and Actuators B: Chemical* **2006,** *114*, (1), 218-222.

15. Alongi, J.; Carosio, F.; Malucelli, G. Layer by layer complex architectures based on ammonium polyphosphate, chitosan and silica on polyester-cotton blends: flammability and combustion behaviour. *Cellulose* **2012,** *19*, (3), 1041-1050.

16. Alongi, J.; Colleoni, C.; Malucelli, G.; Rosace, G. Hybrid phosphorus-doped silica architectures derived from a multistep sol–gel process for improving thermal stability and flame retardancy of cotton fabrics. *Polymer Degradation and Stability* **2012,** *97*, (8), 1334-1344.

17. Carosio, F.; Alongi, J.; Malucelli, G. [small alpha]-Zirconium phosphate-based nanoarchitectures on polyester fabrics through layer-by-layer assembly. *Journal of Materials Chemistry* **2011,** *21*, (28), 10370-10376.

18. Carosio, F.; Alongi, J.; Malucelli, G. Layer by Layer ammonium polyphosphate-based coatings for flame retardancy of polyester–cotton blends. *Carbohydrate Polymers* **2012,** *88*, (4), 1460-1469.

19. Carosio, F.; Laufer, G.; Alongi, J.; Camino, G.; Grunlan, J. C. Layer-by-layer assembly of silica-based flame retardant thin film on PET fabric. *Polymer Degradation and Stability* **2011,** *96*, (5), 745-750.

20. Tang, Z.; Kotov, N. A.; Magonov, S.; Ozturk, B. Nanostructured artificial nacre. *Nature Materials* **2003,** *2*, 413-418.

21. Jang, W.-S.; Rawson, I.; Grunlan, J. C. Layer-by-layer assembly of thin film oxygen barrier. *Thin Solid Films* **2008,** *516*, (15), 4819–4825.

22. Priolo, M. A.; Gamboa, D.; Holder, K. M.; Grunlan, J. C. Super Gas Barrier of Transparent Polymer−Clay Multilayer Ultrathin Films. *Nano Lett.* **2010,** *10*, (12), 4970–4974.

23. Priolo, M. A.; Gamboa, D.; Grunlan, J. C. Transparent Clay−Polymer Nano Brick Wall Assemblies with Tailorable Oxygen Barrier. *ACS Appl. Mater. Interfaces* **2010,** *2*, (1), 312–320.

24. Farhat, T. R.; Hammond, P. T. Designing a New Generation of Proton-Exchange Membranes Using Layer-by-Layer Deposition of Polyelectrolytes. *Advanced Functional Materials* **2005,** *15*, (6), 945-954.

25. Pontié, M.; Ben Rejeb, S.; Legrand, J. Anti-microbial approach onto cationic-exchange membranes. *Separation and Purification Technology* **2012,** *101*, (0), 91-97.

26. Ishigami, T.; Amano, K.; Fujii, A.; Ohmukai, Y.; Kamio, E.; Maruyama, T.; Matsuyama, H. Fouling reduction of reverse osmosis membrane by surface modification via layer-by-layer assembly. *Separation and Purification Technology* **2012,** *99*, (0), 1-7.

27. Jiang, S. P.; Tang, H. Methanol crossover reduction by Nafion modification via layer-by-layer self-assembly techniques. *Colloids and Surfaces A: Physicochemical and Engineering Aspects* **2012,** *407*, 49-57.

28. Zhang, H.; Huang, H.; Shen, P. K. Methanol-blocking Nafion composite membranes fabricated by layer-by-layer self-assembly for direct methanol fuel cells. *International Journal of Hydrogen Energy* **2012,** *37*, (8), 6875-6879.

29. Yılmaztürk, S.; Ercan, N.; Deligöz, H. Influence of LbL surface modification on oxygen cross-over in self-assembled thin composite membranes. *Applied Surface Science* **2012,** *258*, (7), 3139-3146.

30. Deligöz, H.; Yılmaztürk, S.; Yılmazoğlu, M.; Damyan, H. The effect of self-assembled multilayer formation via LbL technique on thermomechanical and transport properties of Nafion®112 based composite membranes for PEM fuel cells. *Journal of Membrane Science* **2010,** *351*, (1–2), 131-140.

31. Saren, Q.; Qiu, C. Q.; Tang, C. Y. Synthesis and Characterization of Novel Forward Osmosis Membranes based on Layer-by-Layer Assembly. *Environmental Science & Technology* **2011,** *45*, (12), 5201-5208.

32. Malaisamy, R.; Talla-Nwafo, A.; Jones, K. L. Polyelectrolyte modification of nanofiltration membrane for selective removal of monovalent anions. *Separation and Purification Technology* **2011,** *77*, (3), 367-374.

33. Li, X. F.; Feyter, S. D.; Vankelecom, I. F. J. Poly(sulfone)/sulfonated poly(ether ether ketone) blend membranes: morphology study and application in the filtration of alcohol based feeds. *Journal of Membrane Science* **2008,** *324*, (1-2), 67-75.

34. Ahmadiannamini, P.; Li, X.; Goyens, W.; Meesschaert, B.; Vanderlinden, W.; Feyter, S. D.; Vankelecom, I. F. J. Influence of polyanion type and cationic counter ion on the SRNF performance of polyelectrolyte membranes. *Journal of Membrane Science* **2012,** *403-404*, 216-226.

35. Torras, C.; Garcia-Valls, R. Quantification of membrane morphology by interpretation of scanning electron microscopy images. *Journal of Membrane Science* **2004,** *233*, (1–2), 119-127.

36. Tylkowski, B.; Trusheva, B.; Bankova, V.; Giamberini, M.; Peev, G.; Nikolova, A. Extraction of biologically active compounds from propolis and concentration of extract by nanofiltration. *Journal of Membrane Science* **2010,** *348*, (1–2), 124-130.

37. Xu, H.; Liu, Q. Spectroscopy characterization of anthracene in SDS/BA/H2O system. *Spectrochimica Acta Part A: Molecular and Biomolecular Spectroscopy* **2008,** *70*, (2), 243-246.

38. Shukla, R.; Cheryan, M. Performance of ultrafiltration membranes in ethanol–water solutions: effect of membrane conditioning. *Journal of Membrane Science* **2002,** *198*, (1), 75-85.

39. Kwon, Y.-N.; Leckie, J. O. Hypochlorite degradation of crosslinked polyamide membranes: II. Changes in hydrogen bonding behavior and performance. *Journal of Membrane Science* **2006,** *282*, (1–2), 456-464.

40. Socrates, G. *Infrared and Raman Characteristic Group Frequencies: Tables and Charts*. John Wiley & Sons: 2004; p 107,125.

41. Chen, S.-H.; Liou, R.-M.; Lai, J.-Y.; Lai, C.-L. Effect of the polarity of additional solvent on membrane formation in polysulfone/N-methyl-2-pyrrolidone/water ternary system. *European Polymer Journal* **2007,** *43*, (9), 3997-4007.

42. Niwa, M.; Kawakami, H.; Kanamori, T.; Shinbo, T.; Kaito, A.; Nagaoka, S. Gas Separation of Asymmetric 6FDA Polyimide Membrane with Oriented Surface Skin Layer. *Macromolecules* **2001,** *34*, (26), 9039-9044.

43. van de Witte, P.; Dijkstra, P. J.; van den Berg, J. W. A.; Feijen, J. Phase separation processes in polymer solutions in relation to membrane formation. *Journal of Membrane Science* **1996,** *117*, (1–2), 1-31.

44. Conesa, A.; Gumí, T.; Palet, C. Membrane thickness and preparation temperature as key parameters for controlling the macrovoid structure of chiral activated membranes (CAM). *Journal of Membrane Science* **2007,** *287*, (1), 29-40.

45. Smolders, C. A.; Reuvers, A. J.; Boom, R. M.; Wienk, I. M. Microstructures in phase-inversion membranes. Part 1. Formation of macrovoids. *Journal of Membrane Science* **1992,** *73*, (2–3), 259-275.

46. Termonia, Y. Fundamentals of polymer coagulation. *Journal of Polymer Science Part B: Polymer Physics* **1995,** *33*, (2), 279-288.

47. Yang, Y.-H.; Haile, M.; Park, Y. T.; Malek, F. A.; Grunlan, J. C. Super Gas Barrier of All-Polymers Multilayers Thin Films. *Macromolecules* **2011,** *44*, 1450-1459.

48. Wavhal, D. S.; Fisher, E. R. Modification of polysulfone ultrafiltration membranes by CO2 plasma treatment. *Desalination* **2005,** *172*, (2), 189-205.

49. Smallwood, I. M. *Handbook of Organic Solvent Properties*. Butterworth- Heinemann: 1996.

50. Yang, X. J.; Livingston, A. G.; Freitas dos Santos, L. Experimental observations of nanofiltration with organic solvents. *Journal of Membrane Science* **2001,** *190*, (1), 45-55.

51. Machado, D. o. R.; Hasson, D.; Semiat, R. Effect of solvent properties on permeate flow through nanofiltration membranes. Part I: investigation of parameters affecting solvent flux. *Journal of Membrane Science* **1999,** *163*, (1), 93-102.

52. Bhanushali, D.; Kloos, S.; Kurth, C.; Bhattacharyya, D. Performance of solvent-resistant membranes for non-aqueous systems: solvent permeation results and modeling. *Journal of Membrane Science* **2001,** *189*, (1), 1-21.

53. Buonomenna, M. G.; Golemme, G.; Jansen, J. C.; Choi, S. H. Asymmetric PEEKWC membranes for treatment of organic solvent solutions. *Journal of Membrane Science* **2011,** *368*, (1–2), 144-149.

54. Schmidt, P.; Köse, T.; Lutze, P. Characterisation of organic solvent nanofiltration membranes in multi-component mixtures: Membrane rejection maps and membrane selectivity maps for conceptual process design. *Journal of Membrane Science* **2013,** *429*, (0), 103-120.

55. Zhao, Y.; Yuan, Q. Effect of membrane pretreatment on performance of solvent resistant nanofiltration membranes in methanol solutions. *Journal of Membrane Science* **2006,** *280*, (1–2), 195-201.

56. Bonnet, J. L.; Guiraud, P.; Dusser, M.; Kadri, M.; Laffosse, J.; Steiman, R.; Bohatier, J. Assessment of anthracene toxicity toward environmental eukaryotic microorganisms: Tetrahymena pyriformis and selected micromycetes. *Ecotoxicology and Environmental Safety* **2005,** *60*, (1), 87-100.

57. Lane, D. A., Polycyclic Aromatic Hydrocarbons: Atmospheric Physics and Chemistry. In *Organic Chemistry of the Atmosphere*, L.D. Hansen, D. J. E., Ed. CRC Press: Florida, 1991; pp 155-198.

58. Su, B.; Wang, T.; Wang, Z.; Gao, X.; Gao, C. Preparation and performance of dynamic layer-by-layer PDADMAC/PSS nanofiltration membrane. *Journal of Membrane Science* **2012,** *423–424*, (0), 324-331.

59. Barton, A. F. M. *Handbook of Solubility Parameters*. CRC Press: 1983.